Supplementary Material (ESI) for New Journal of Chemistry

Supporting Information for

Highly Stable Blue Light-Emitting Materials with a Three-Dimensional Architecture: Improvement of Charge Injections and Electroluminescence Performance

Ting Lei, Jia Luo, Lei Wang, Yuguo Ma, Jian Wang, Yong Cao, and Jian Pei

Beijing National Laboratory for Molecular Sciences (BNLMS) Key Labs of Bioorganic Chemistry and Molecular Engineering and of Polymer Chemistry, College of Chemistry, Peking University, Beijing 100871 and Institute of Polymer Optoelectronic Materials and Devices, and Key Lab of Specially Functional Materials of Ministry of Education Department, South China University of Technology, Guangzhou 510640, China

Table of Contents

1. Molecular model of **sFCbz**.

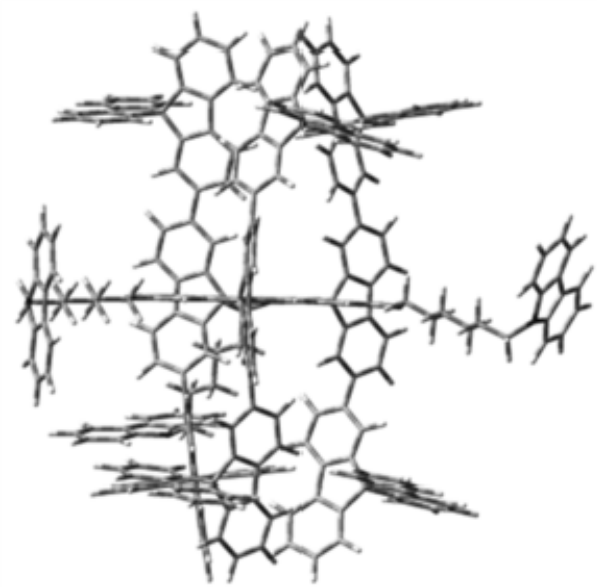

Figure S1 The energy was minimized at PM3 level using Gaussian 03 packages

2. UV and PL Spectra of **F** series.

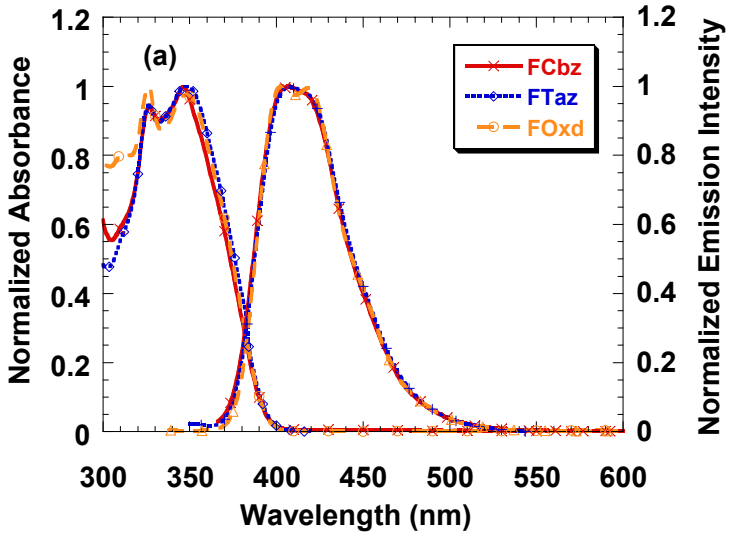

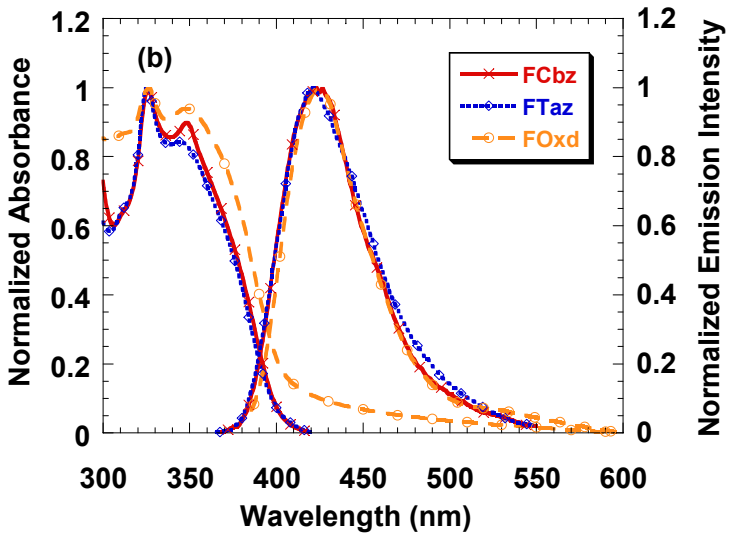

Figure S2 The normalized absorption and PL spectra of **F** series: (a) in dilute toluene solutions (1×10^{-6} M); (b) in solid state (spin casting from toluene).

3. PL Spectra of **sFOxd** and **FOxd** at Different Exciting Wavelength

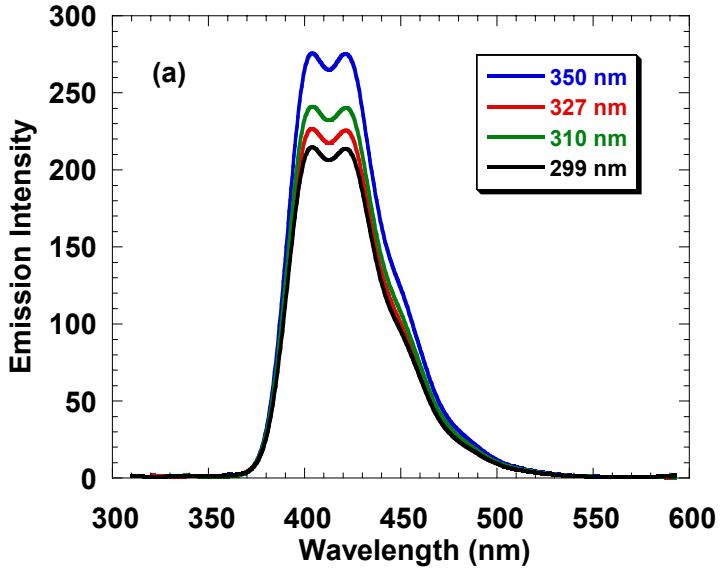

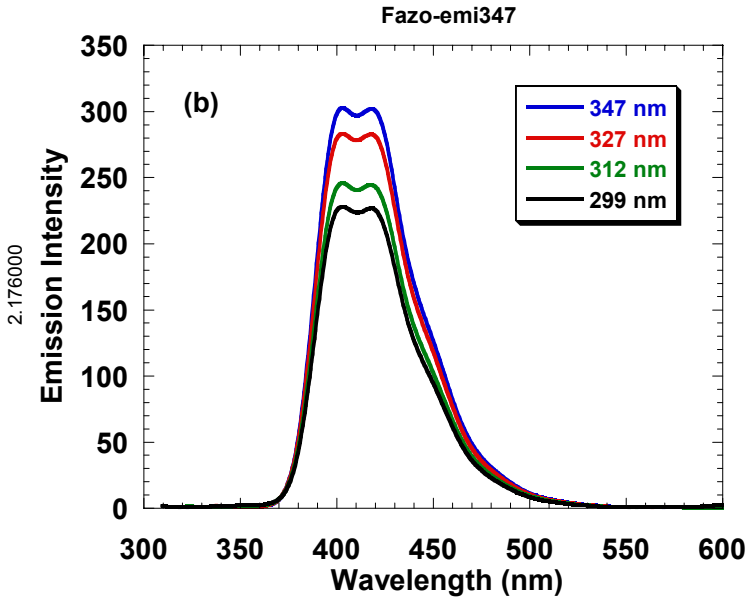

Figure S3 PL spectra of **sFOxd** and **FOxd** at different exciting wavelength (350 nm, 327 nm, 310 nm, 299 nm) in dilute solution (1×10^{-6} M, toluene). The excitations at the absorption of the **Oxd** groups (299 nm and 310 nm) show completely the emission of the congujaged arms, which indicate the efficient intramolecular energy transfer.

4. Cyclic Voltammograms Spectra of **F** series.

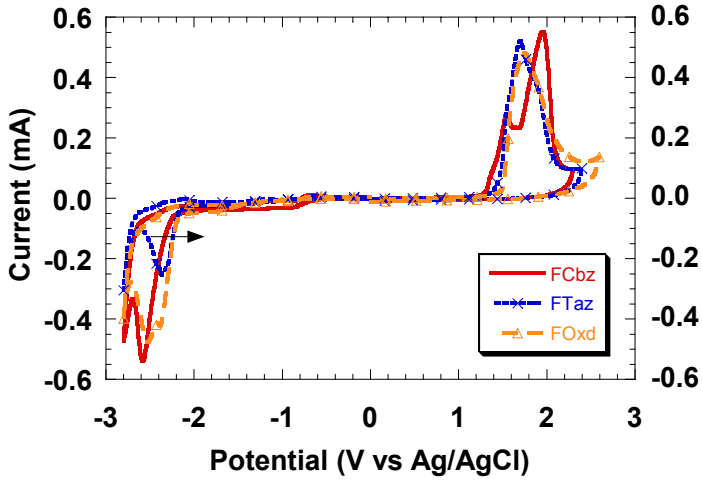

Figure S4 Cyclic voltammograms of drop-cast films of the **F** series. Scan rate, 100 $mV\bullet s^{-1}$; working electrode, glassy carbon; auxiliary electrode, Pt wire; reference electrode, Ag/AgCl; supporting electrolyte *n*-Bu_4NPF_6 (0.1 M, CH_3CN). The black arrow indicates the onset changes of the three compounds.

5. Thermal Properties .

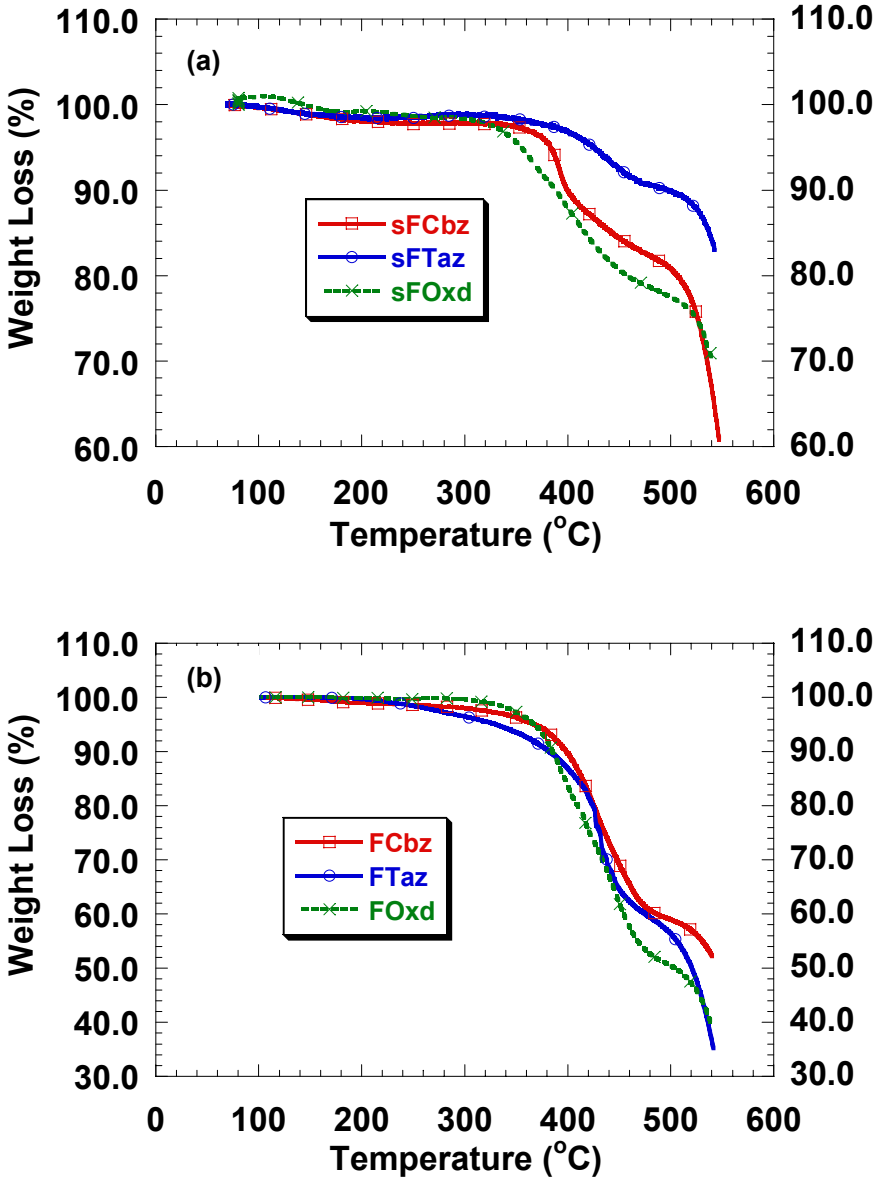

Figure S5 TGA curves of (a) **sF** series and (b) **F** series in nitrogen atmosphere at a heating rate of 10 °C/min.

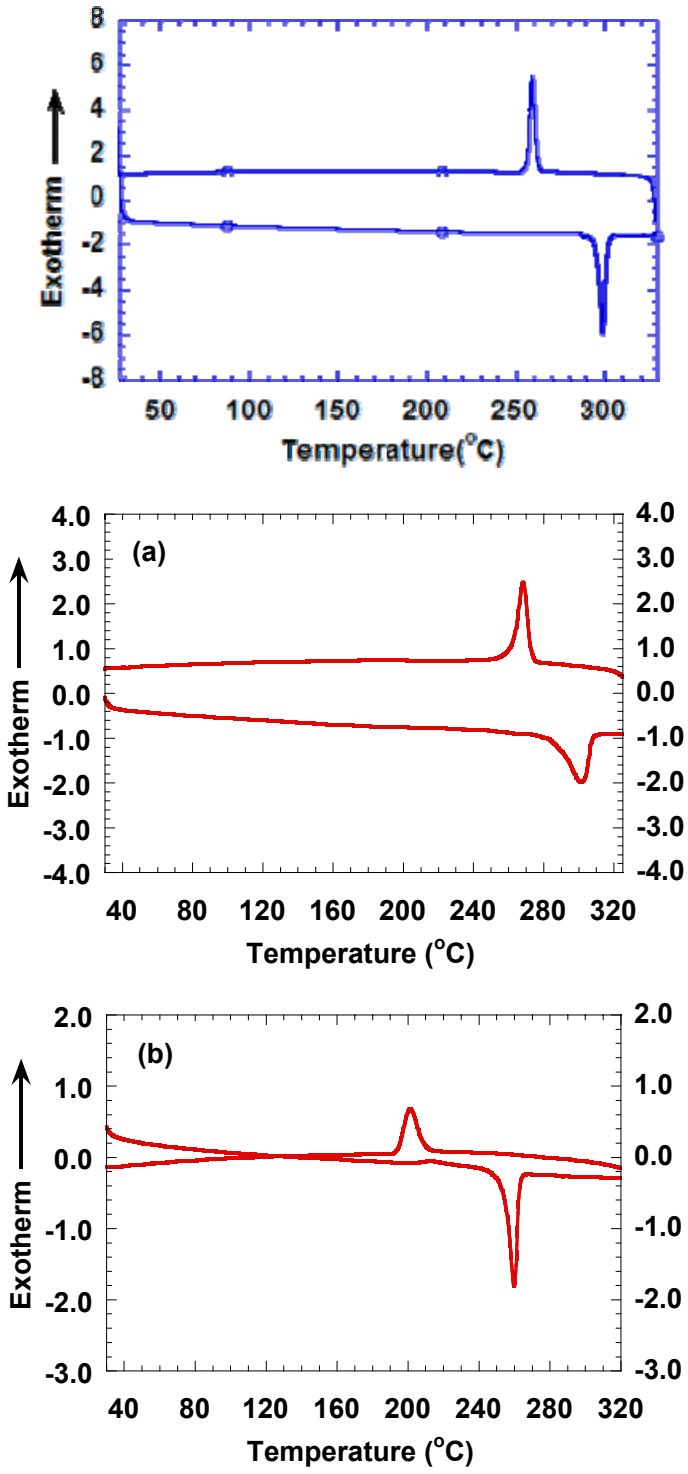

Figure S6 DSC traces of (a)**FCbz** , (b) **FTaz**and (c) **FOxd** recorded at a heating rate of 10 °C min^{-1}.

6. Surface Morphologies of **sFCbz**, **FCbz**, **sFOxd** and **FOxd**:

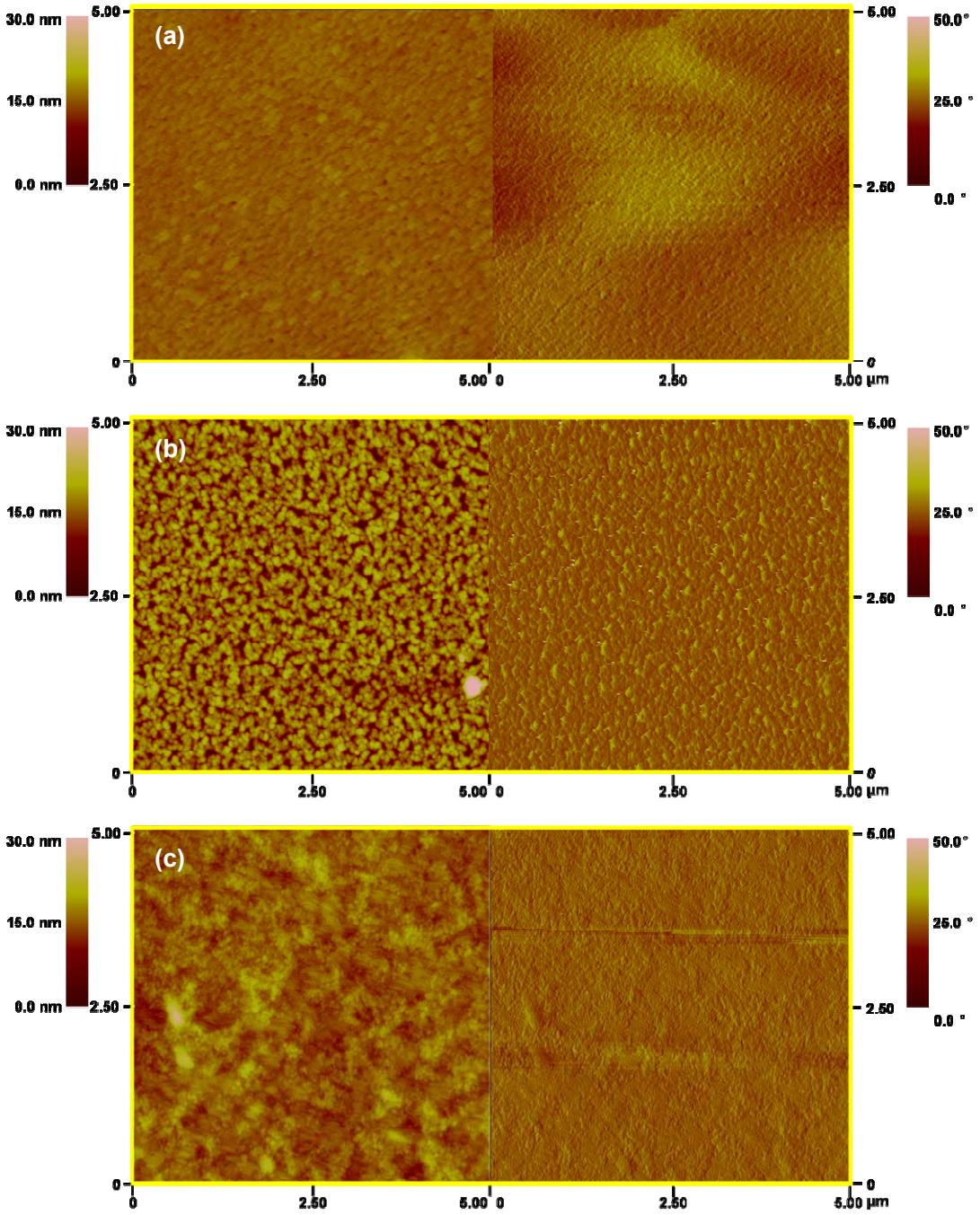

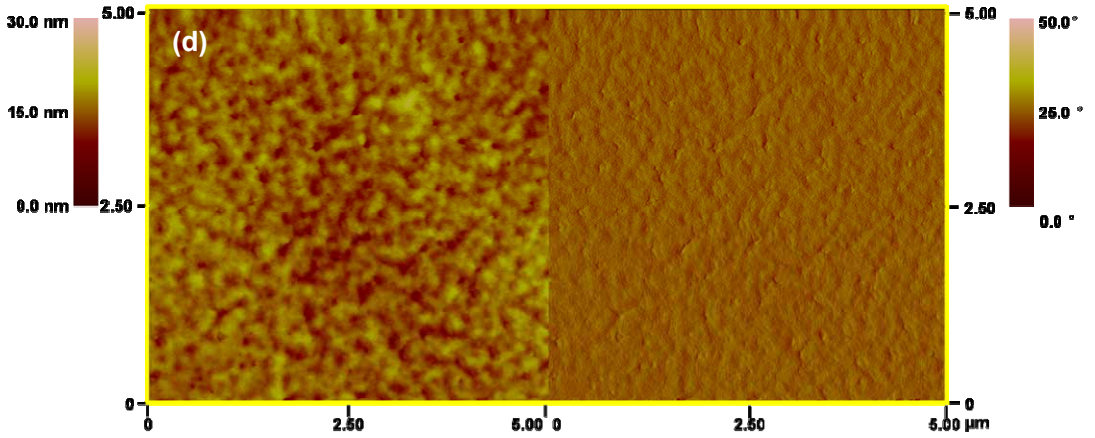

Figure S7 Tapping-mode AFM height images and phase images of (a) **sFCbz** (5×5μm), (b) **FCbz** (5×5μm), (c) **sFOxd** (5×5μm) and (d) **FOxd** (5×5μm) in thin film (spin-casted on quartz plane from 5 mg/mL toluene solution). As indicated by the height images, the **sF series** exhibit better amorphous morphologies than **F series**. The phase images, which are more sensitive to the grain edges, also show that the **F series** have a strong tendency to crystallize.

7. J-LE characteristics of double-layer devices

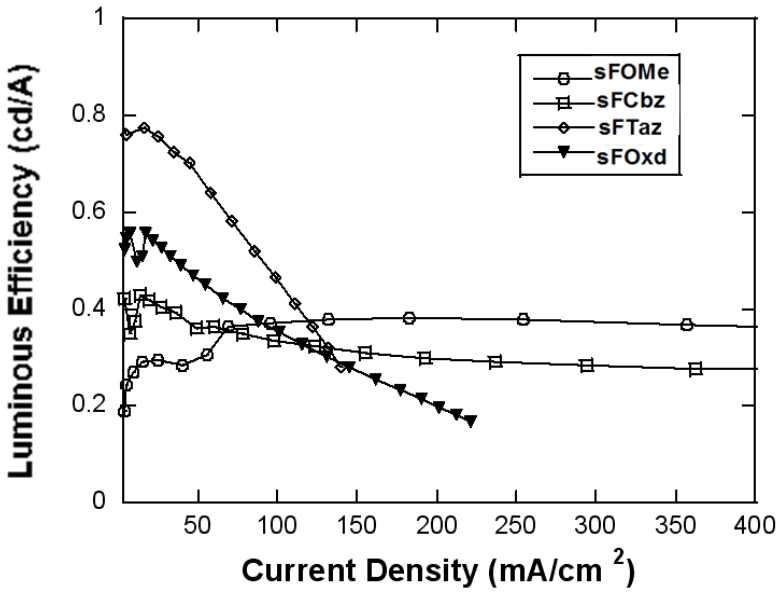

Figure S8. J-LE characteristics of double-layer devices: ITO/PEDOT/PVK /EL/Ba/Al.

8. EL spectra Stability of compounds **sFCbz** and **sFOxd**

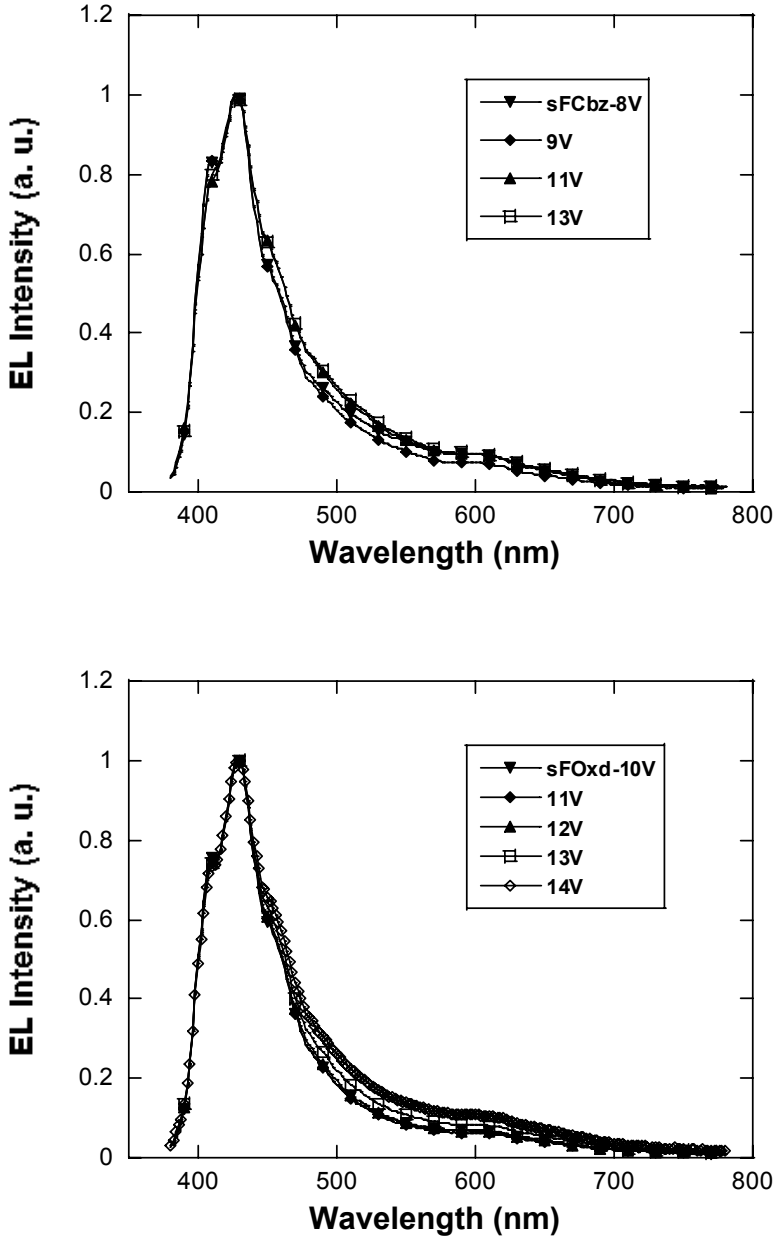

Figure S9 Electroluminescence spectra of **sFCbz** and **sFOxd** with device structure ITO/PEDOT/PVK/EL/Ba/Al under increasing bias.

9. ^{1}H and ^{13}C NMR Spectra

Compound **9**

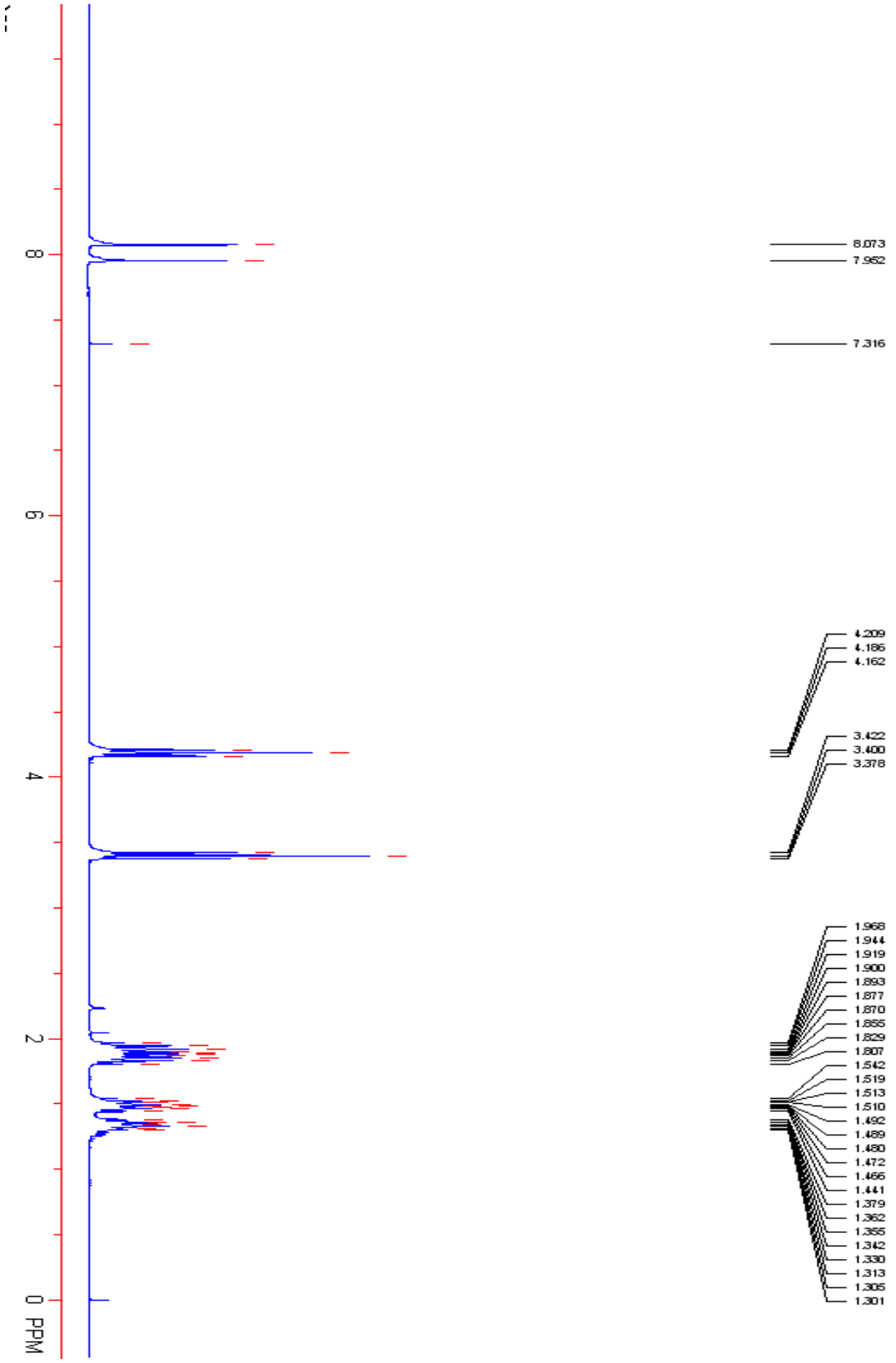

Compound **9**

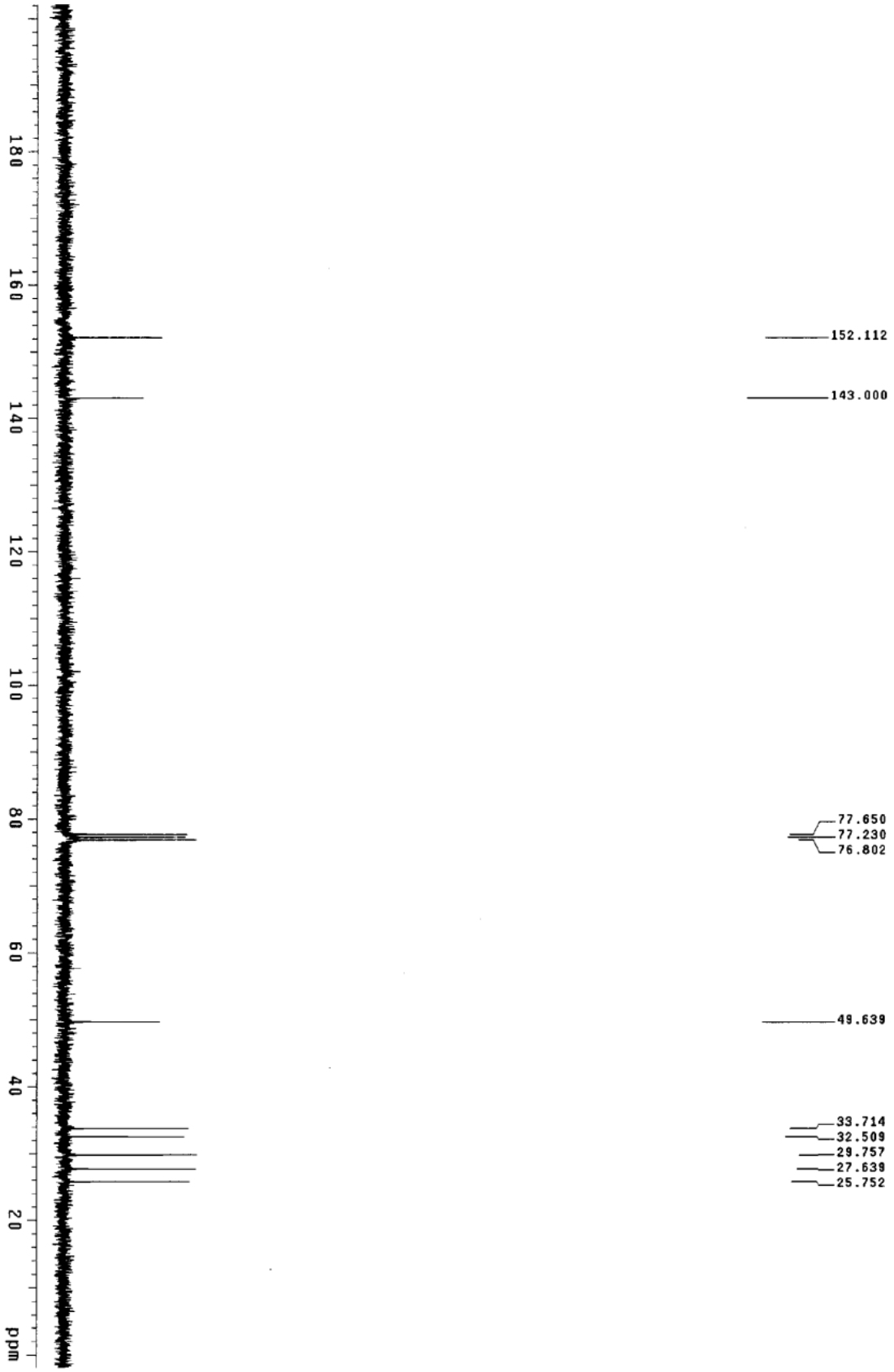
180
160
140
120
100
80
60
40
20
ppm
152.112
143.000
77.650
77.230
76.802
49.639
33.714
32.509
29.757
27.639
25.752

Compound **sFOH**

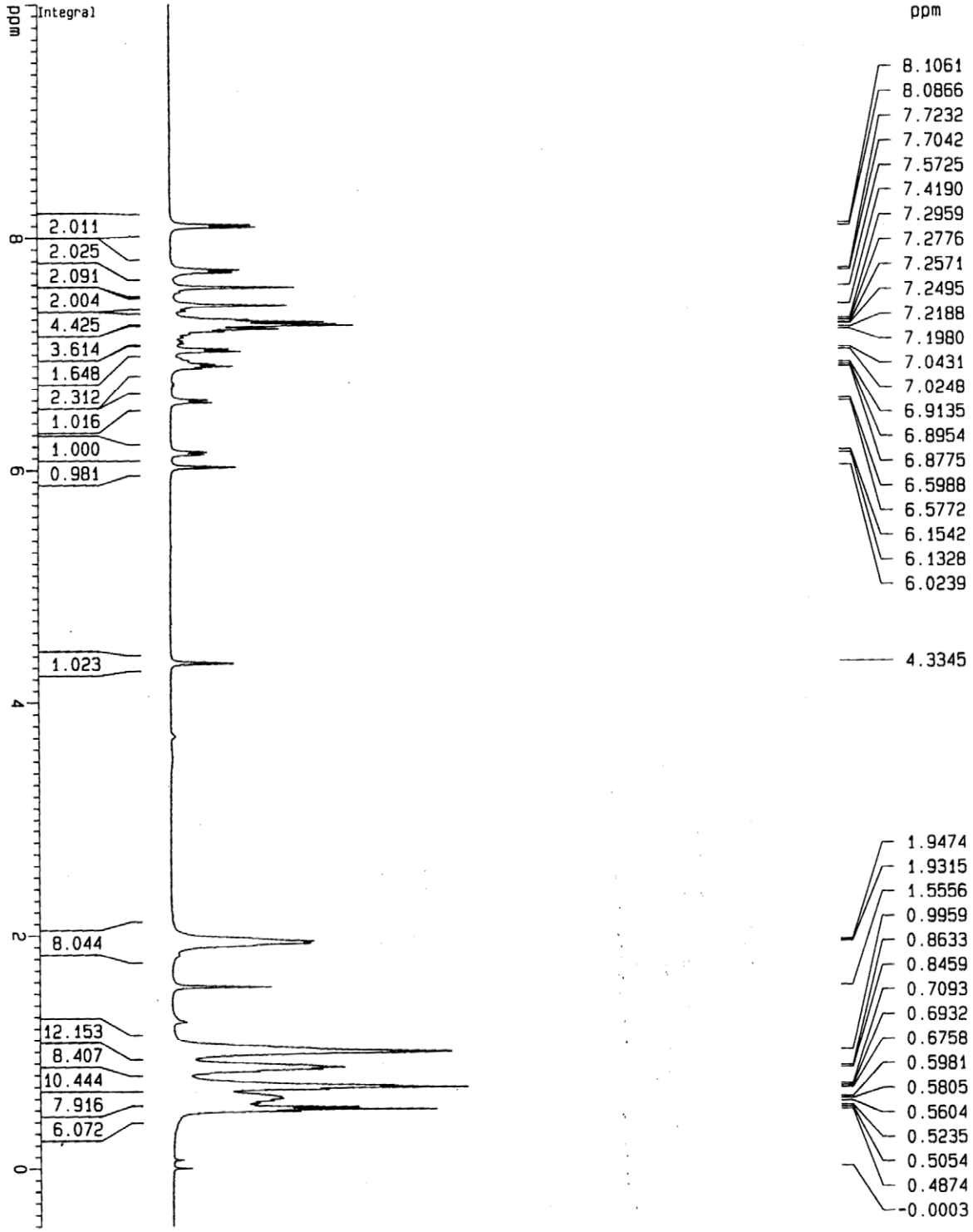

Compound **sFOH**

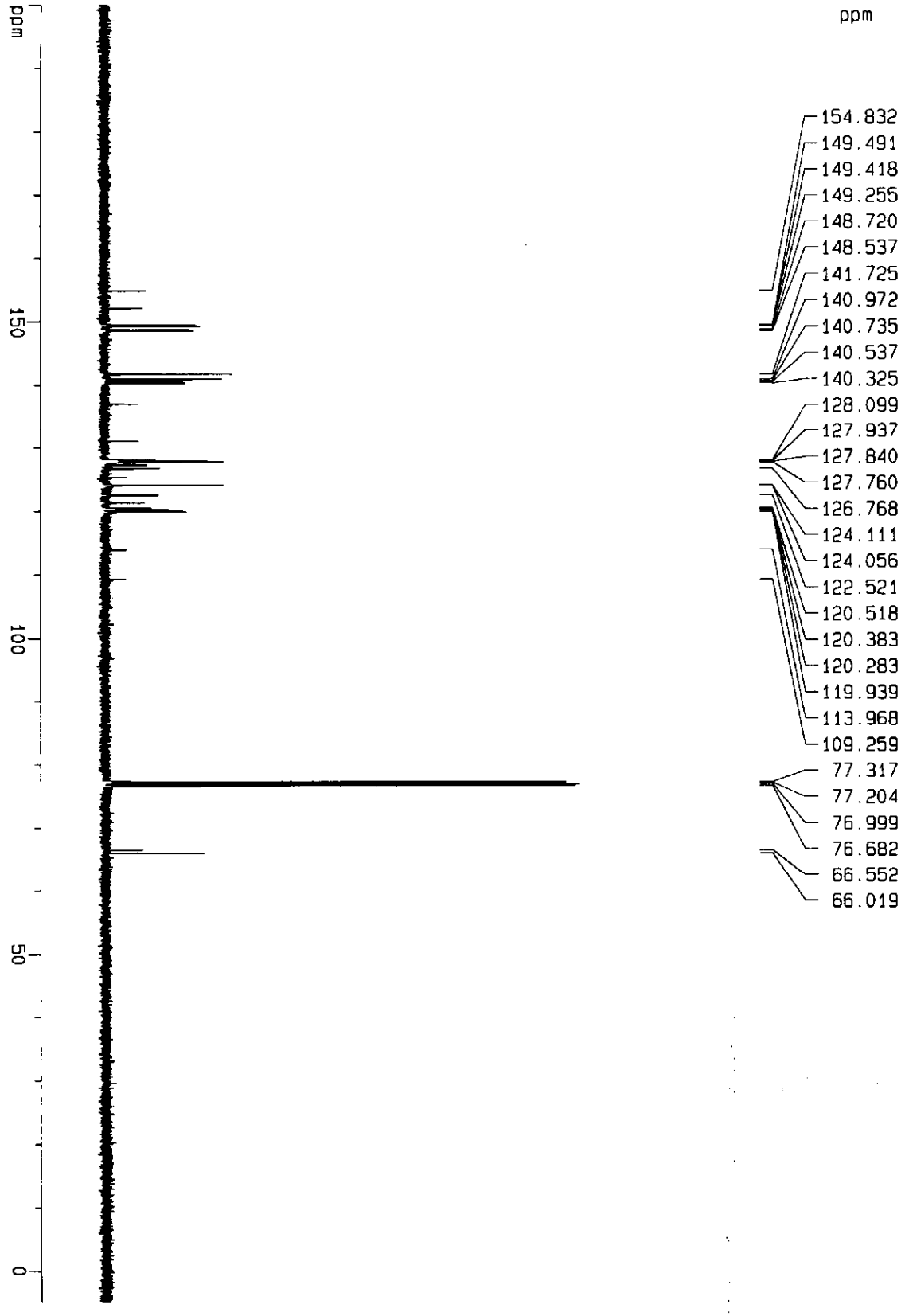

Compound **FOH**

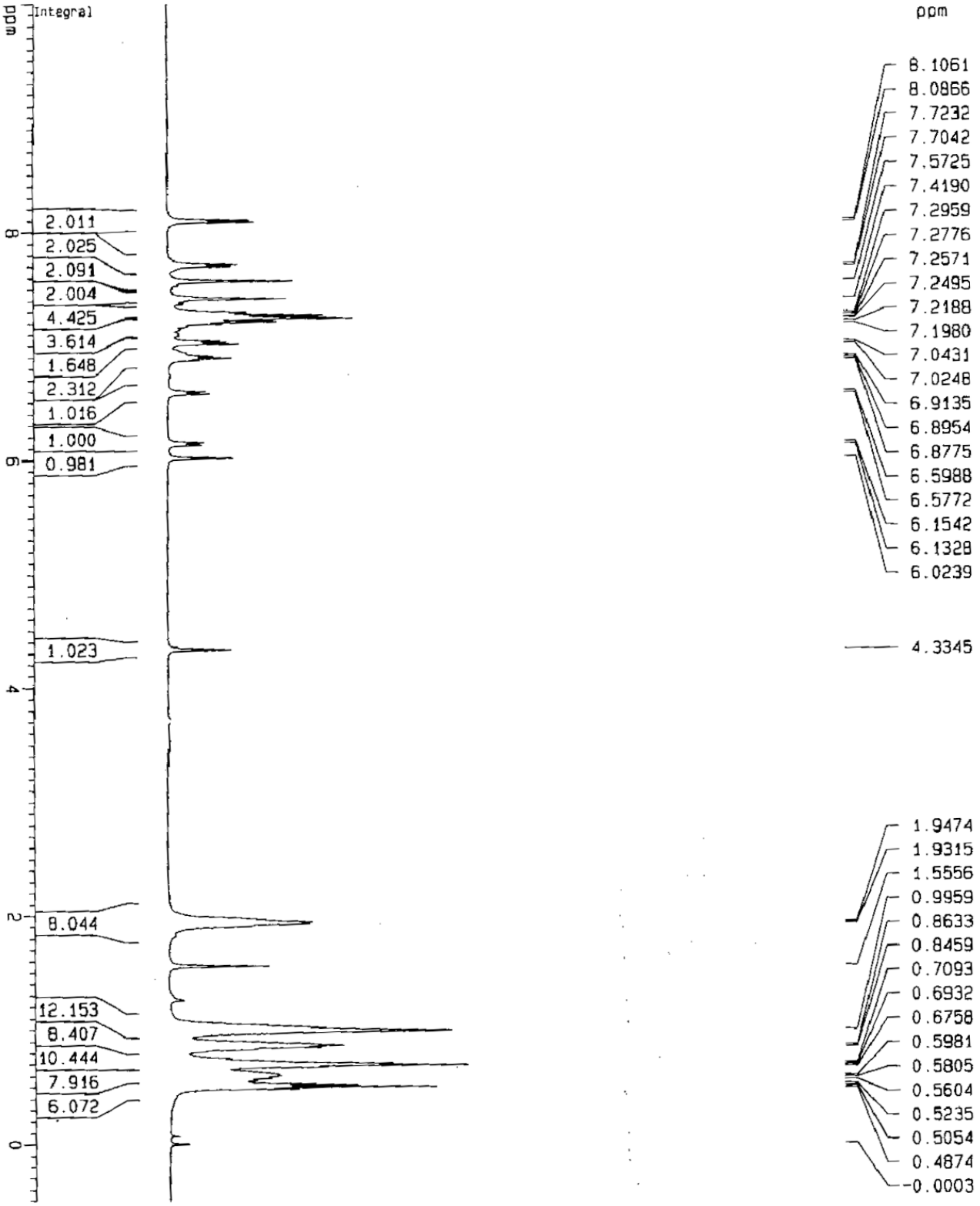

Compound **FOH**

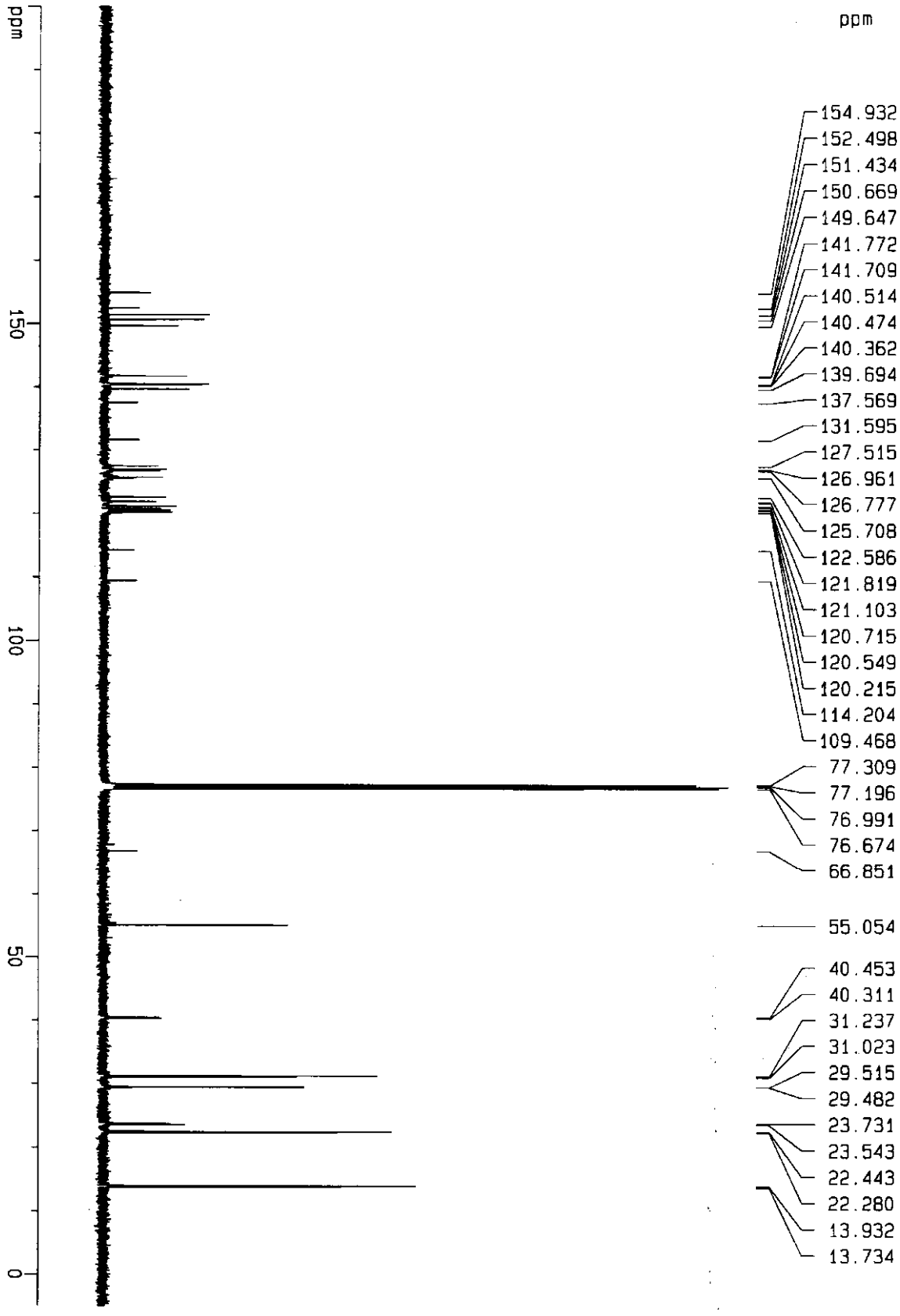
ppm
150
100
50
0
ppm
154.932
152.498
151.434
150.669
149.647
141.772
141.709
140.514
140.474
140.362
139.694
137.569
131.595
127.515
126.961
126.777
125.708
122.586
121.819
121.103
120.715
120.549
120.215
114.204
109.468
77.309
77.196
76.991
76.674
66.851
55.054
40.453
40.311
31.237
31.023
29.515
29.482
23.731
23.543
22.443
22.280
13.932
13.734

Compound **sFCbz**

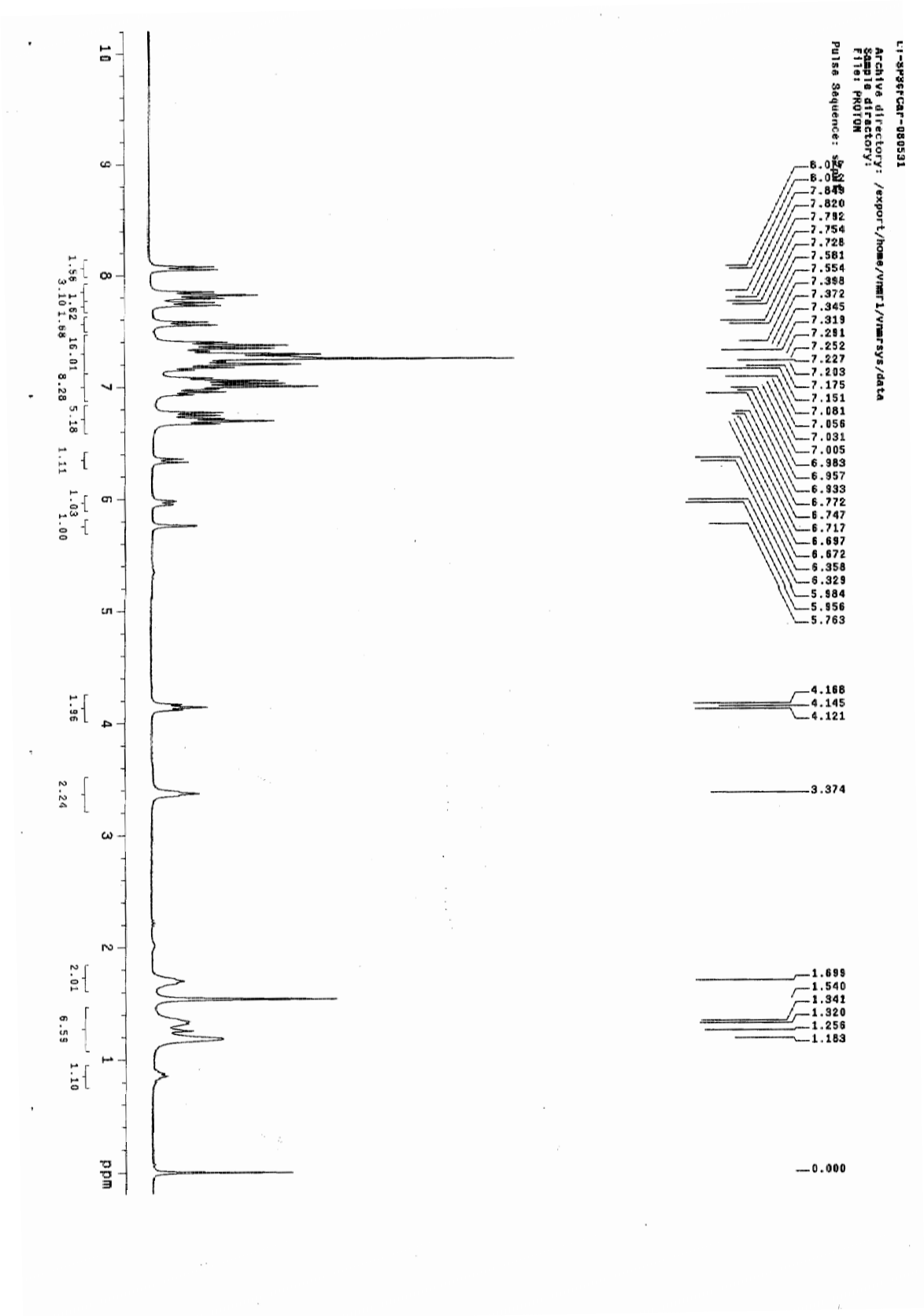

Compound **sFCbz**

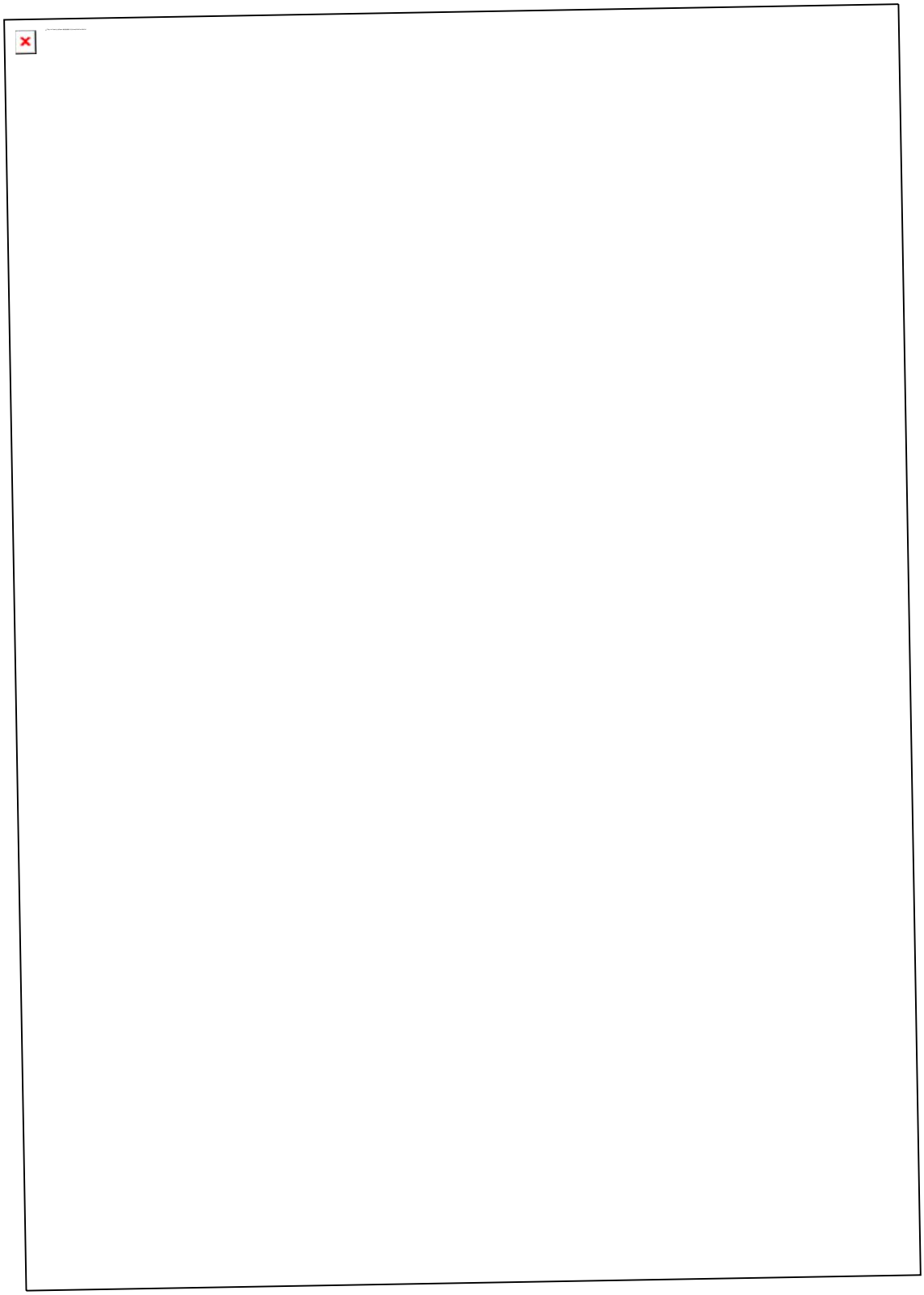

Compound **sFTaz**

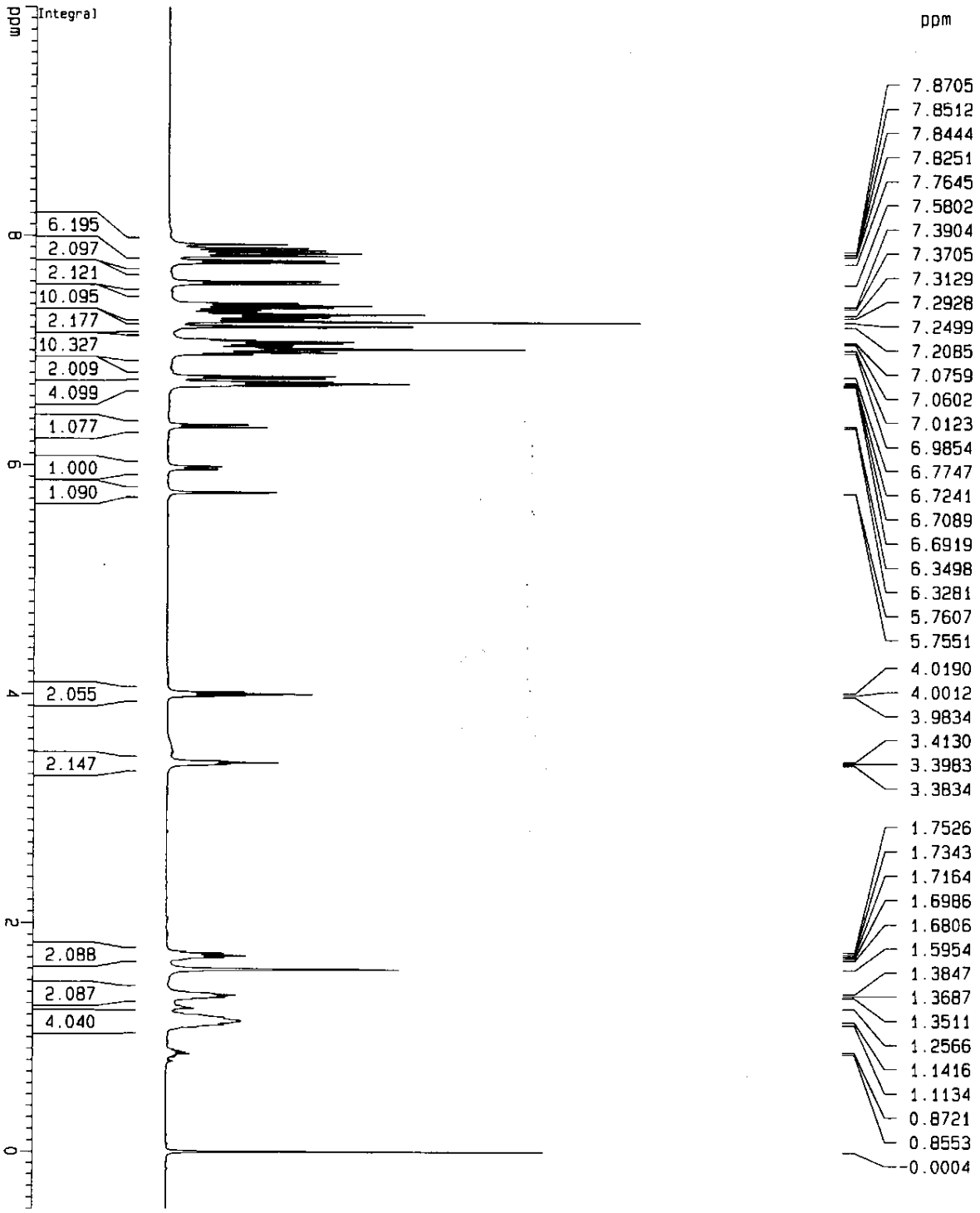

Compound **sFTaz**

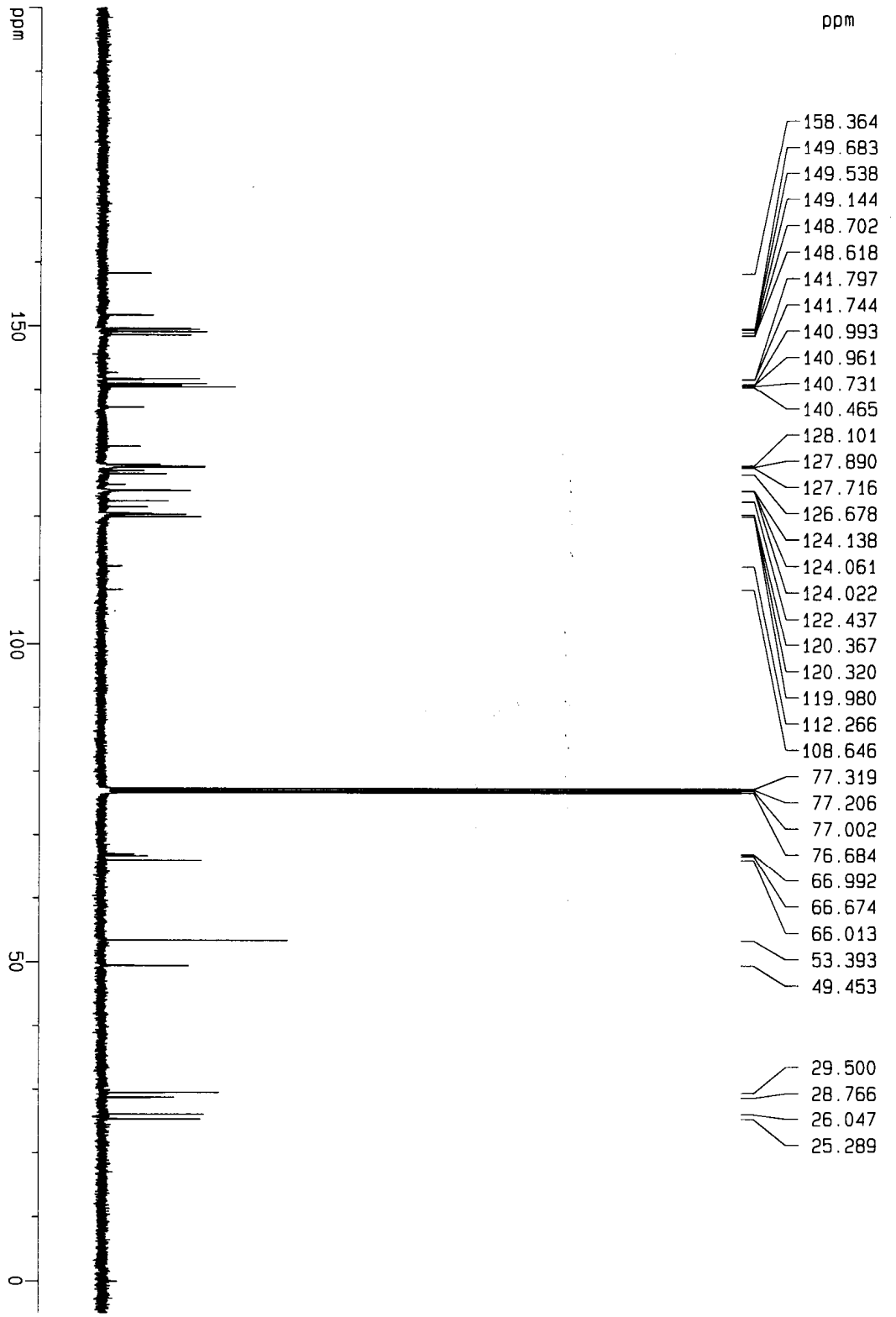
ppm
150
100
50
0
ppm
158.364
149.683
149.538
149.144
148.702
148.618
141.797
141.744
140.993
140.961
140.731
140.465
128.101
127.890
127.716
126.678
124.138
124.061
124.022
122.437
120.367
120.320
119.980
112.266
108.646
77.319
77.206
77.002
76.684
66.992
66.674
66.013
53.393
49.453
29.500
28.766
26.047
25.289

Compound **sFOxd**

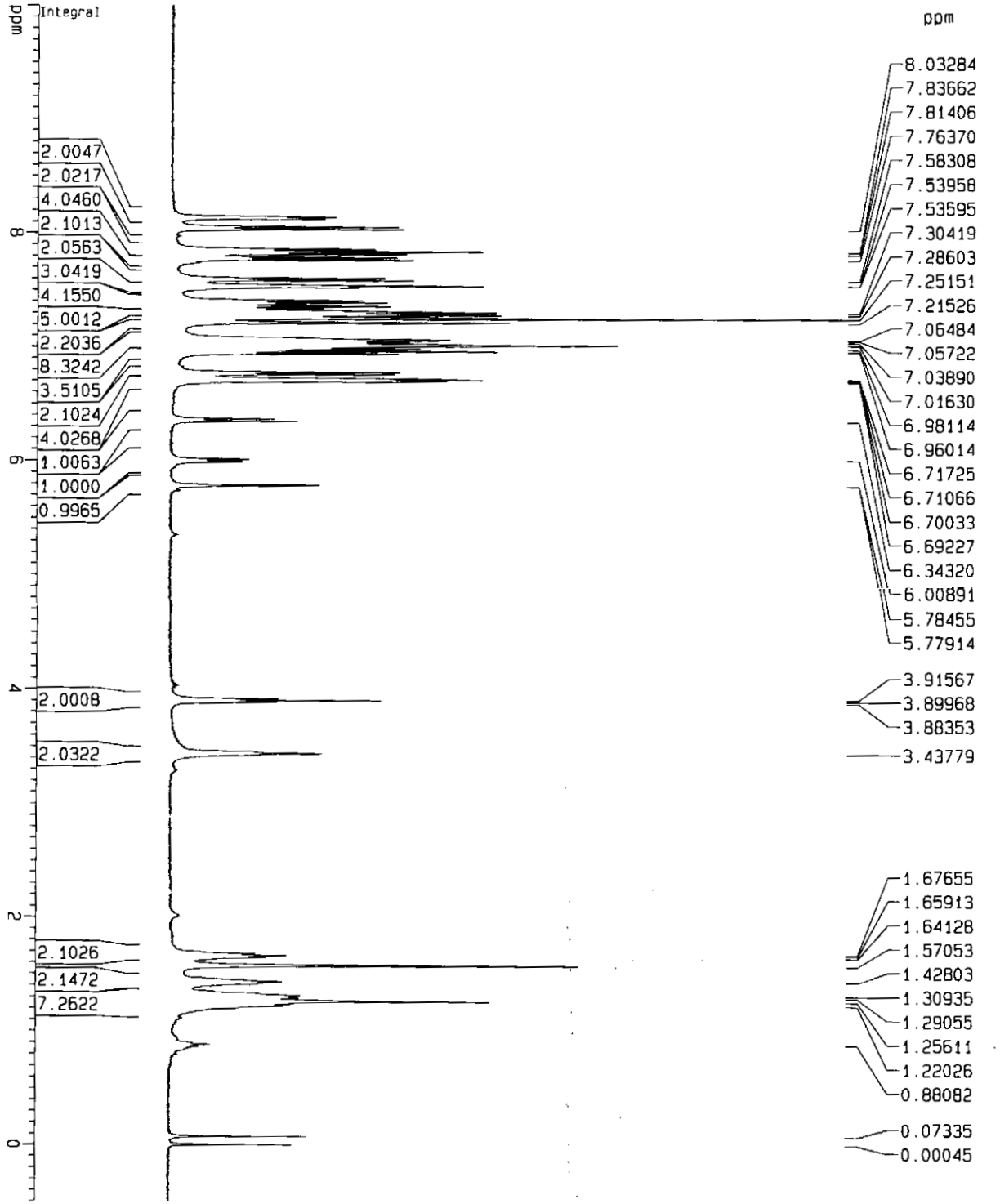

Compound **sFOxd**

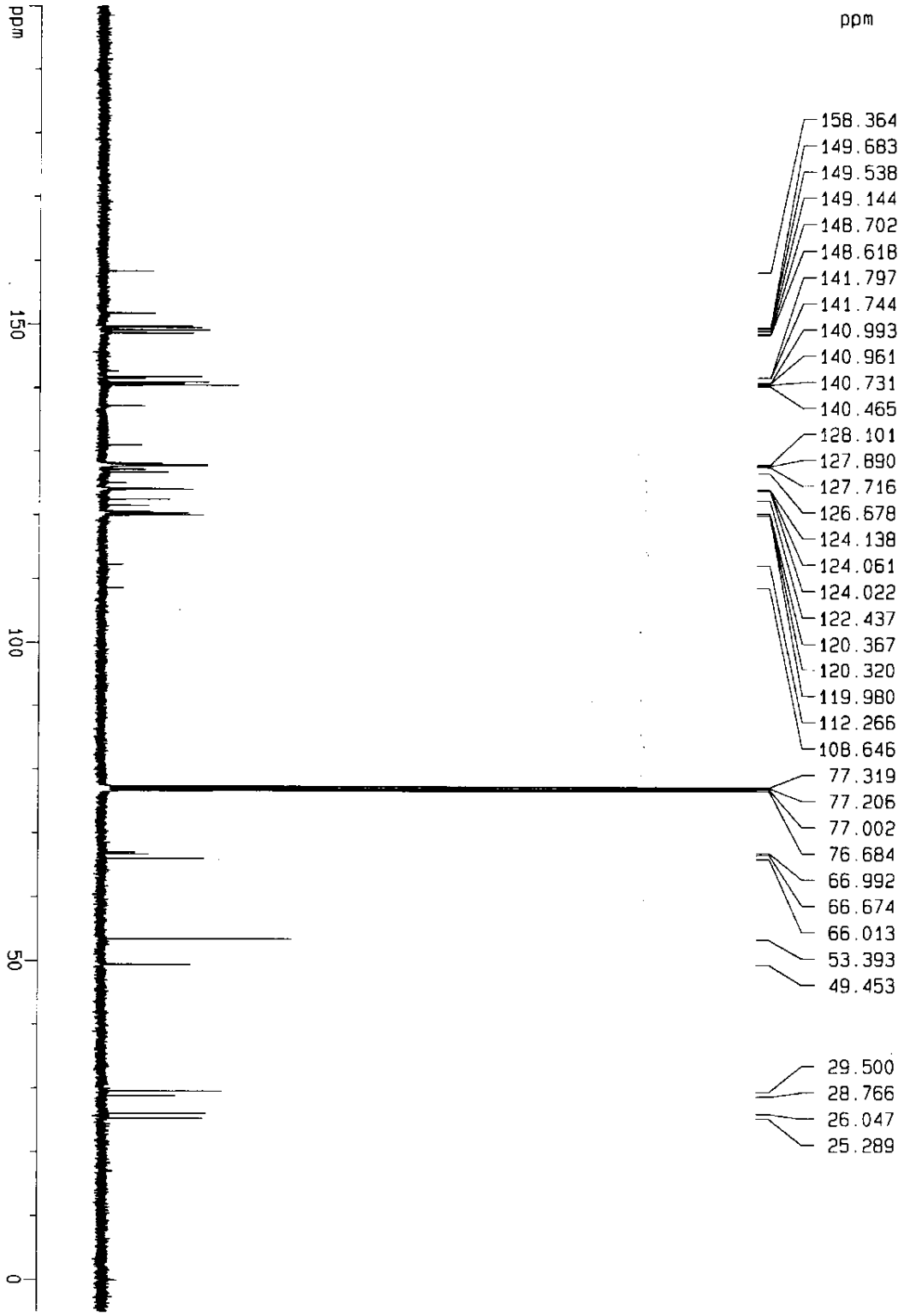

Compound **FCbz**

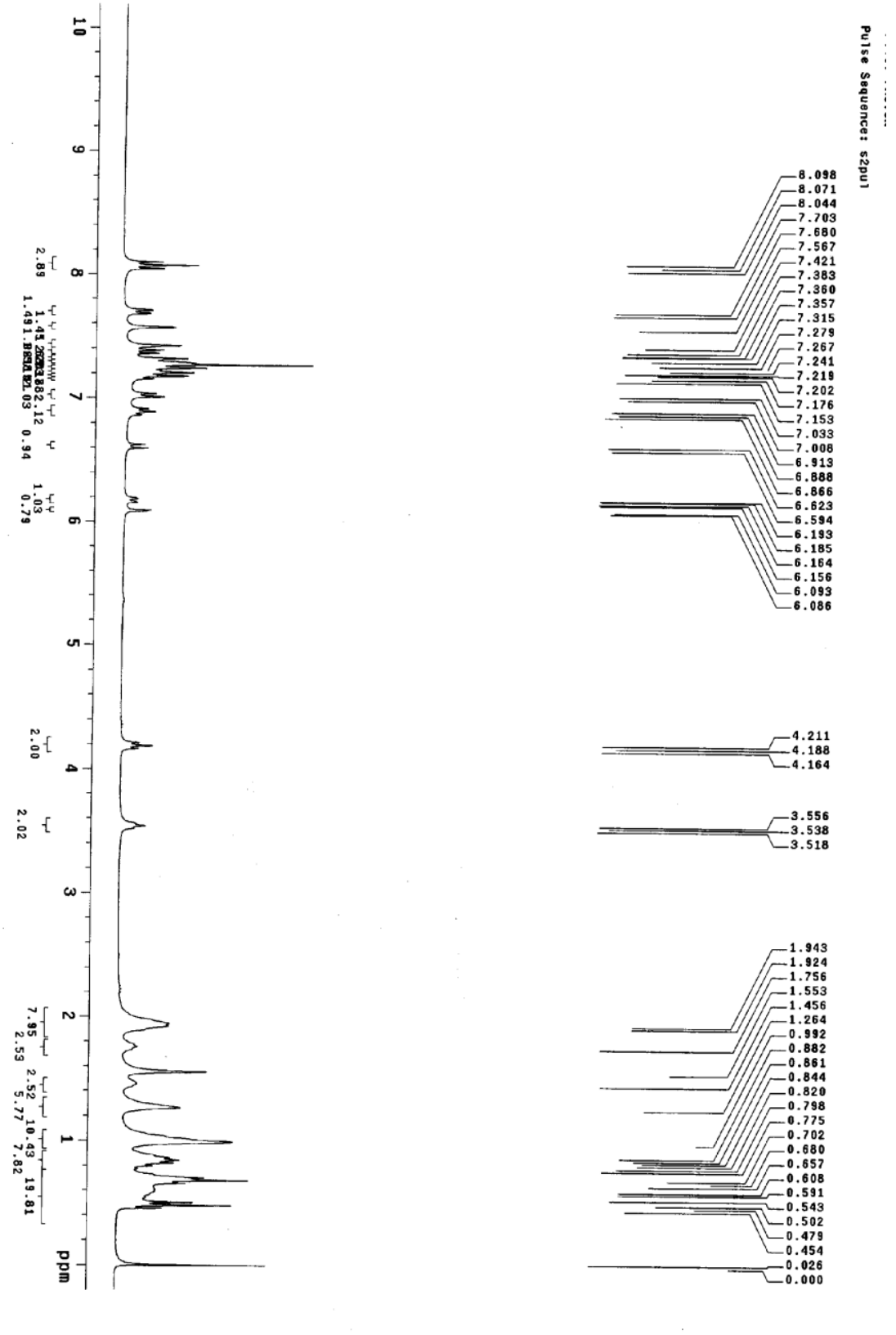

Compound **FCbz**

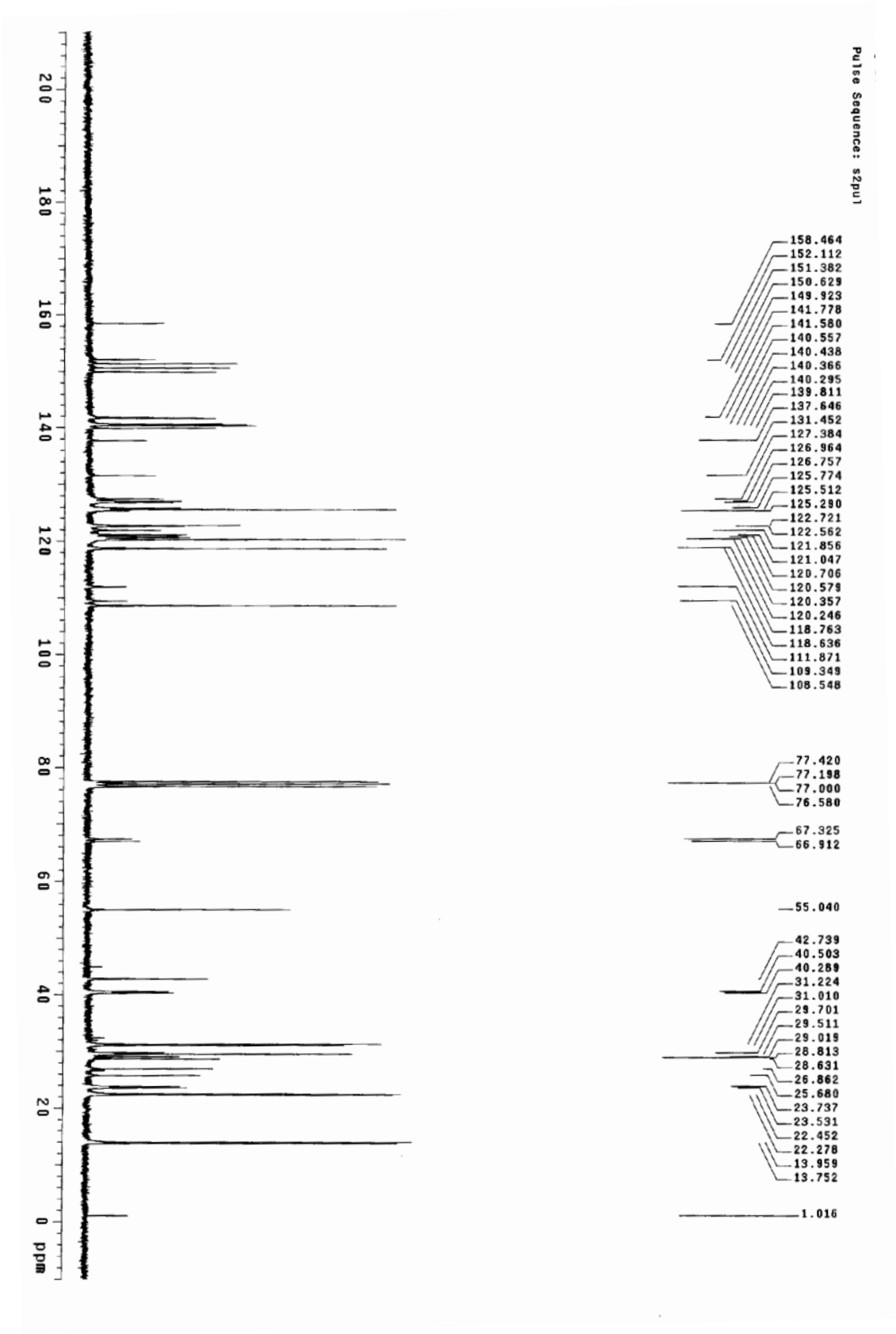
Pulse Sequence: s2pul
158.464
152.112
151.382
150.629
149.923
141.778
141.580
140.557
140.438
140.366
140.295
139.811
137.646
131.452
127.384
126.964
126.757
125.774
125.512
125.280
122.721
122.562
121.856
121.047
120.706
120.579
120.357
120.246
118.763
118.636
111.871
109.349
108.548
77.420
77.198
77.000
76.580
67.325
66.912
55.040
42.739
40.503
40.289
31.224
31.010
29.701
29.511
29.019
28.813
28.631
26.862
25.680
23.737
23.531
22.452
22.278
13.959
13.752
1.016
200
180
160
140
120
100
80
60
40
20
0 ppm

Compound **FTaz**

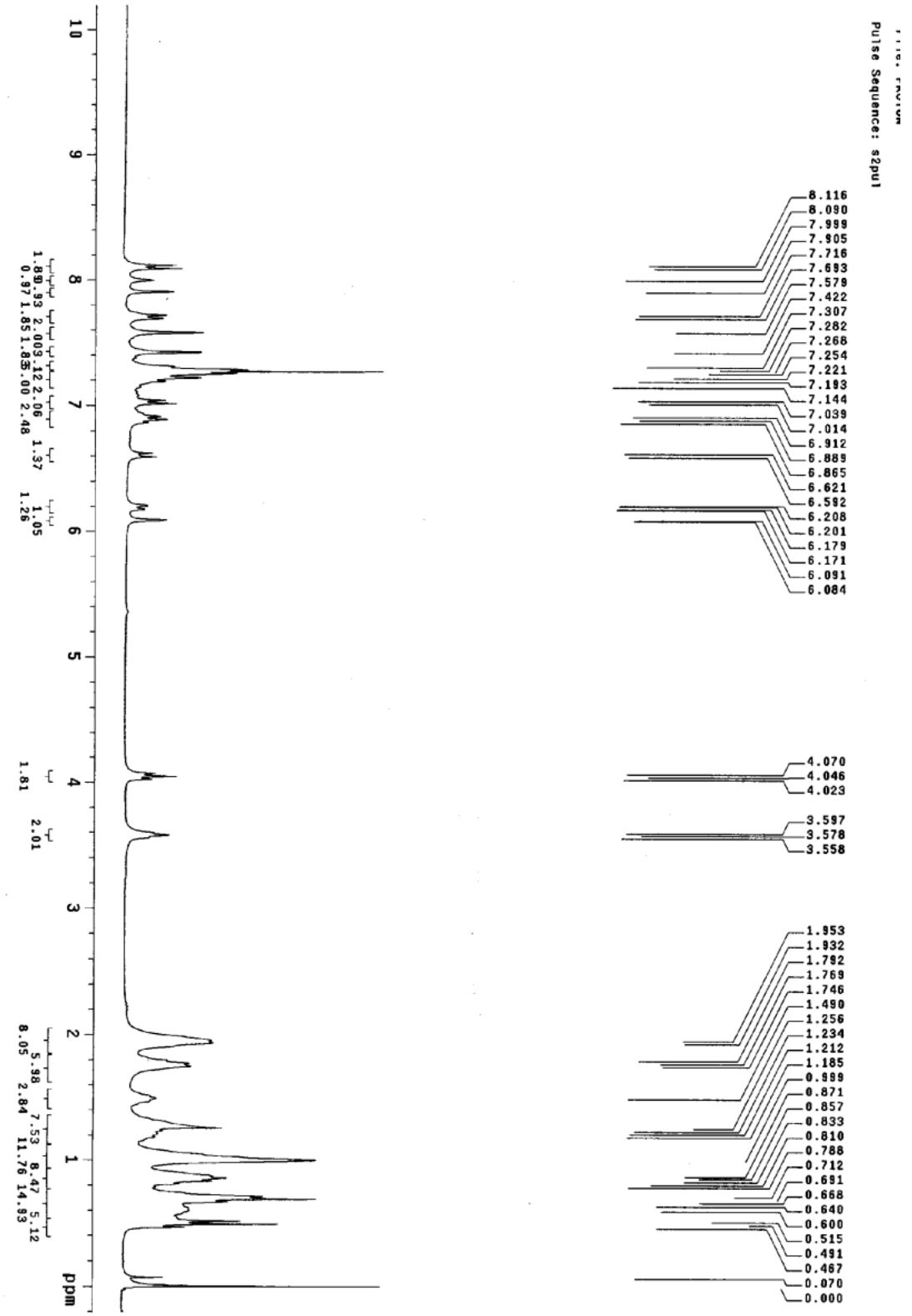

Compound **FTaz**

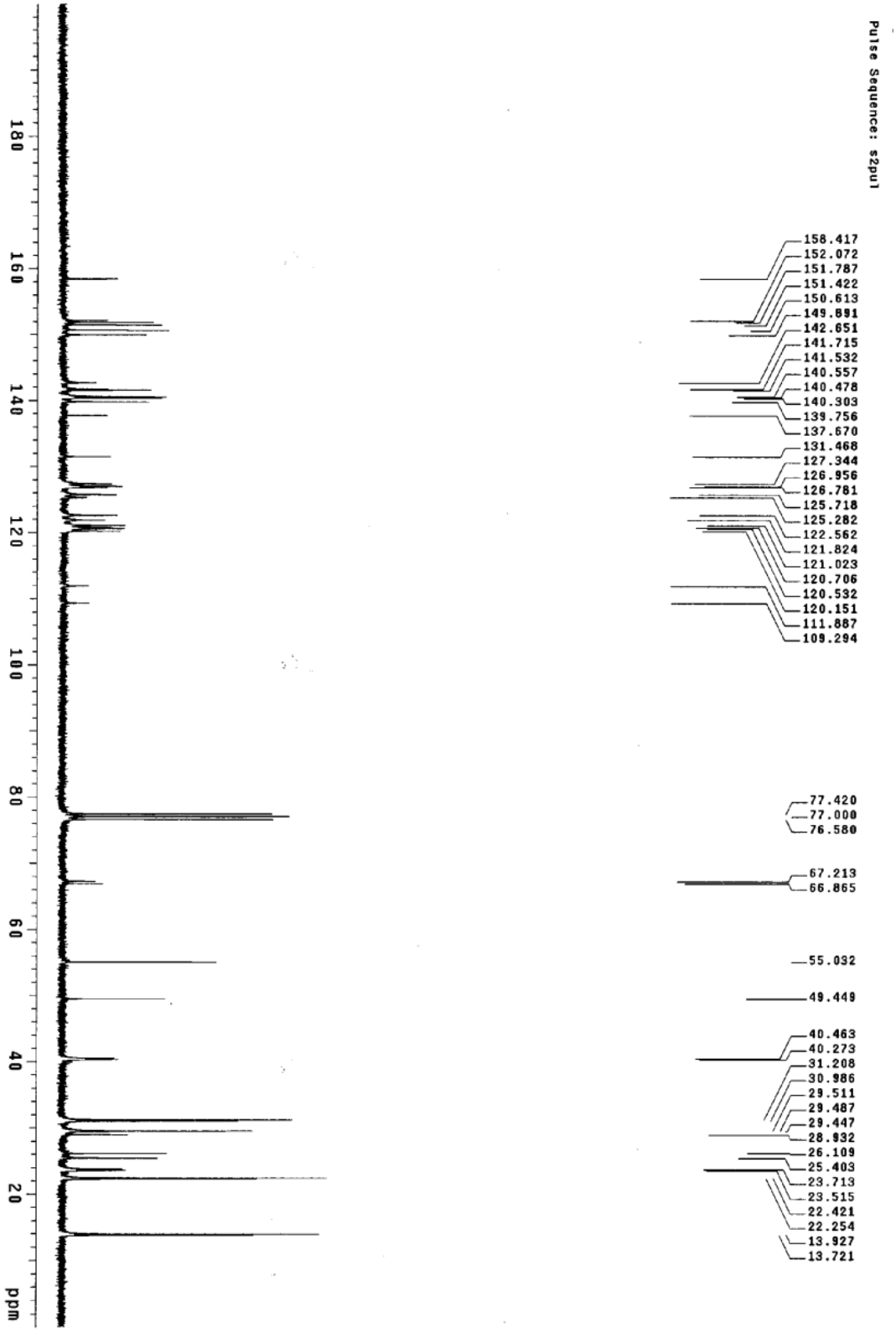

Compound **FOxd**

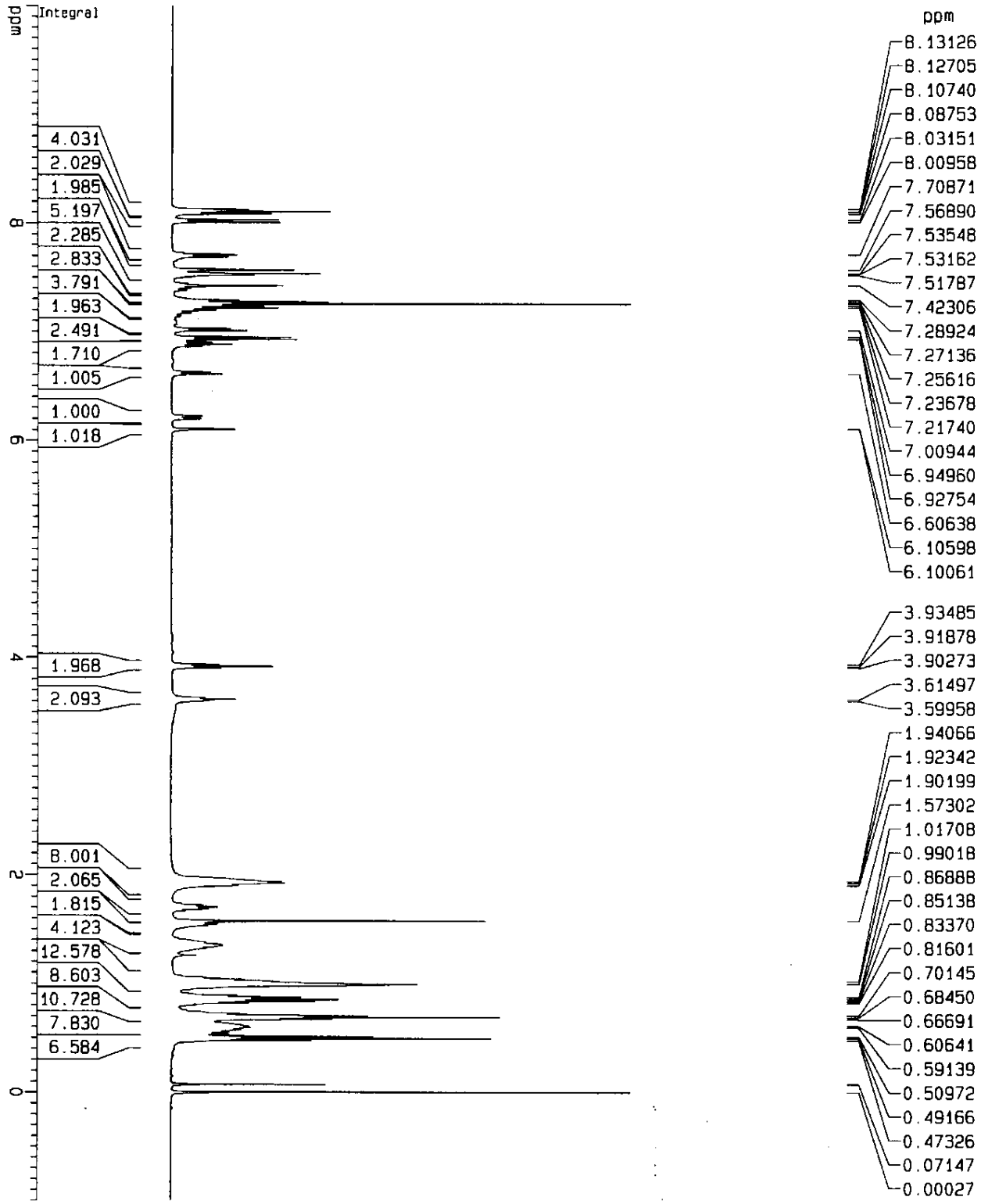

Compound **FOxd**